

Investigation on intergranular exchange coupling effect in Pr₉Fe_{85.5}B_{5.5} ribbons

Z. B. Li, M. Zhang, L. C. Wang, B. G. Shen, X. F. Zhang, Y. F. Li, F. X. Hu, and J. R. Sun

Citation: [Applied Physics Letters](#) **104**, 052406 (2014); doi: 10.1063/1.4863749

View online: <http://dx.doi.org/10.1063/1.4863749>

View Table of Contents: <http://scitation.aip.org/content/aip/journal/apl/104/5?ver=pdfcov>

Published by the [AIP Publishing](#)

Articles you may be interested in

[Enhanced refrigerant capacity in two-phase nanocrystalline/amorphous NdPrFe₁₇ melt-spun ribbons](#)

Appl. Phys. Lett. **104**, 212401 (2014); 10.1063/1.4879544

[Origin of recoil hysteresis in nanocomposite Pr₈Fe₈₇B₅ magnets](#)

J. Appl. Phys. **113**, 013902 (2013); 10.1063/1.4772606

[Coercivity enhancement in Pr_{9.5}Fe₈₃Zr₂B_{5.5} magnetic nanomaterials](#)

J. Appl. Phys. **112**, 073924 (2012); 10.1063/1.4758314

[The microstructure and magnetization behaviors of \(Pr_{8.2}Fe_{86.1-x}Co_xB_{5.7}\)_{0.99}Zr_{0.01} \(x=0–10\) nanocomposite magnets](#)

J. Appl. Phys. **109**, 07A756 (2011); 10.1063/1.3566074

[Effects of as-quenched structures on the phase transformations and magnetic properties of melt-spun Pr₇Fe₈₈B₅ ribbons](#)

J. Appl. Phys. **86**, 7010 (1999); 10.1063/1.371787

Confidently measure down to 0.01 fA and up to 10 PΩ

Keysight B2980A Series Picoammeters/Electrometers

[View video demo](#)



KEYSIGHT TECHNOLOGIES

Investigation on intergranular exchange coupling effect in $\text{Pr}_9\text{Fe}_{85.5}\text{B}_{5.5}$ ribbons

Z. B. Li,^{1,2} M. Zhang,¹ L. C. Wang,¹ B. G. Shen,^{1,a)} X. F. Zhang,^{2,3} Y. F. Li,^{2,3} F. X. Hu,¹ and J. R. Sun¹

¹State Key Laboratory for Magnetism, Institute of Physics, Chinese Academy of Sciences, Beijing 100190, China

²Key Laboratory of Integrated Exploitation of Bayan Obo Multi-Metal Resources, Inner Mongolia University of Science and Technology, Baotou 014010, China

³School of Mathematics, Physics and Biological Engineering, Inner Mongolia University of Science and Technology, Baotou 014010, China

(Received 9 November 2013; accepted 17 January 2014; published online 4 February 2014)

The intergranular exchange coupling effects are investigated via thermal activation of magnetization reversal in the magnetic relaxation process, combined with Henkel plots and the measurement of susceptibilities in three types of $\text{Pr}_9\text{Fe}_{85.5}\text{B}_{5.5}$ ribbons. Exchange interaction between hard-hard grains is proposed in optimal melt-spun ribbons, as well as in over melt-spun ribbons even bearing a weak exchange coupling between soft-hard grains. In under melt-spun ribbons, the decoupled effect is proposed between hard-hard grains. These investigations may contribute to a clear understanding about the complicated nature of the intergranular exchange coupling in nanocomposite magnets.

© 2014 AIP Publishing LLC. [<http://dx.doi.org/10.1063/1.4863749>]

Nanocomposite magnets have a giant energy product,¹ which theoretically owes to the exchange coupling between magnetically hard phase with high coercivity and soft phase bearing high saturation magnetization.^{2–7} The effect of exchange coupling varies widely due to its strong dependence on the intrinsic interfacial nature, grain size, exchange coefficient, and magnetocrystalline anisotropy.^{8–16} Actually, exchange coupling exists not only between soft-hard grains resulting in a strong resistance against magnetization reversal in soft grains¹ but also between hard-hard grains leading to more uniform magnetization behaviors.¹⁷ The intergranular exchange coupling effect, even investigated extensively, remains unclear to some degree due to its complicated feature in nanocomposite magnets.

Owing to the intergranular exchange coupling effect, magnetization is more reversible, and reversible magnetization reversal is founded not only in soft grains but also in hard grains.^{18,19} Thermal activation of magnetization reversal in the reversible magnetization process originates from magnetization reversal in hard grains, since the exchange coupling energy overcomes the energy barrier with the driving of thermal fluctuation,²⁰ which shed a new light to probe the exchange coupling effect. Henkel plots are also used to check the exchange coupling effect in isotropic nanostructured magnets.^{21,22} In this paper, we investigate the intergranular exchange interaction via thermally activated process, combined with Henkel plot and the measurement of susceptibility in three types of $\text{Pr}_9\text{Fe}_{85.5}\text{B}_{5.5}$ ribbons. It is expected that these investigations may contribute to a better understanding of the exchange coupling effect in nanocomposites with a hybrid structure.

$\text{Pr}_2\text{Fe}_{14}\text{B}/\alpha\text{-Fe}$ ribbons with a nominal composition of $\text{Pr}_9\text{Fe}_{85.5}\text{B}_{5.5}$ were obtained by melt spinning method. The

ingot was melted by induction melting in a quartz tube, and then the melt was ejected onto the surface of a rotating copper wheel by pressurized argon atmosphere. The surface velocity of copper wheel was varied for optimizing the magnetic properties. The samples prepared in melt spinning at wheel surface velocities of 20.5 m/s, 21.5 m/s, and 23 m/s were selected as under (sample A), optimal (sample B), and over melt-spun sample (sample C), respectively. The phase compositions were examined by x-ray diffraction (XRD) using $\text{Cu K}\alpha$ radiation and grain sizes were derived by Scherrer formula. Magnetic measurements were performed using superconducting quantum interference device (SQUID) vibrating sample magnetometer (VSM) at the temperature of 300 K.

The XRD patterns of samples A, B, and C are displayed in Fig. 1(a). All of the samples show a mixture of $\alpha\text{-Fe}$ and isotropic $\text{Pr}_2\text{Fe}_{14}\text{B}$ structure phases. Compared with those in sample A, the intensities of diffraction peaks are a little low in sample B, and some peaks nearly disappear. This result is an indication of finer grains and implies a small fraction of residual interfacial amorphous phase at grain boundary. It is believed that exchange coupling at interface is enhanced owing to the amorphous grain boundaries.^{9–11} In sample C, owing to the higher quenching rate in melt spinning, the content of residual interfacial amorphous phase is a little more than in sample B. According to Scherrer formula, it is estimated that the average grain sizes of $\text{Pr}_2\text{Fe}_{14}\text{B}$ in samples A, B, and C are 21.9, 17.5, and 16.8 nm, respectively, and those of $\alpha\text{-Fe}$ are 18.7, 16.4, and 15.3 nm, respectively. Accordingly, the magnetic properties are different among the three samples.

Fig. 1(b) shows the hysteresis loops for samples A, B, and C at the temperature of 300 K. The squareness of demagnetization curve in second quadrant is better for sample B than for samples A and C, which implies well exchange coupling existing in the optimal melt-spun ribbons and weak

^{a)}Author to whom correspondence should be addressed. Electronic mail: shenbg@iphy.ac.cn

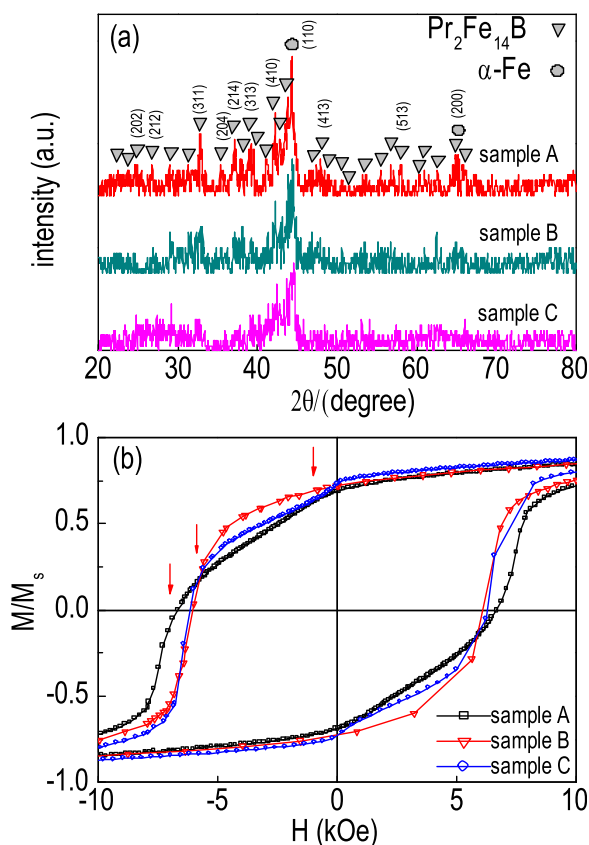


FIG. 1. The XRD patterns of samples A, B, and C (a). The hysteresis loops for samples A, B, and C at the temperature of 300 K (b).

exchange coupling in under and over melt-spun ribbons. Although the magnetic properties are investigated in melt-spun ribbons in a large amount of experiments, the exchange interactions cannot be explained between soft-hard grains alone, and they are believed to be different in a large extent even both weak in under and over melt-spun ribbons.

Owing to exchange interaction the magnetization is more reversible.²³ With this in mind, we could probe the exchange coupling effects in a different method. In this method, first, after magnetized to saturation in positive direction, a negative field H_R is applied on the sample, and then the field is cycled to 0 kOe and kept fixed for a waiting time of 300 s. The inset in Fig. 2 shows the magnetization versus the waiting time in the magnetic relaxation process after the field is cycled from -6.4 kOe. Fig. 2 shows the dependences of ΔM_{active} on field H_R . Here, ΔM_{active} denotes the value of magnetization reversal in the process of keeping the field fixed at zero for 300 s. The values of ΔM_{active} are larger in samples B and C than in sample A, which is supposed to originate from the difference of exchange coupling effects in these samples.

The magnetization reversal in magnetic relaxation results from thermal activation over energy barrier.²⁴⁻³⁰ The anisotropy energy in soft grain is very weak, so the energy barrier is due to the larger magnetocrystalline anisotropy in hard grains. In the remanence state, the magnetization is non-uniform in some hard grains, and a disorder magnetic structure exists within some soft grain.³¹ So there exists the reversed domain, but the energy barrier is at hard grain interface hindering the domain wall motion.³²⁻³⁵ In

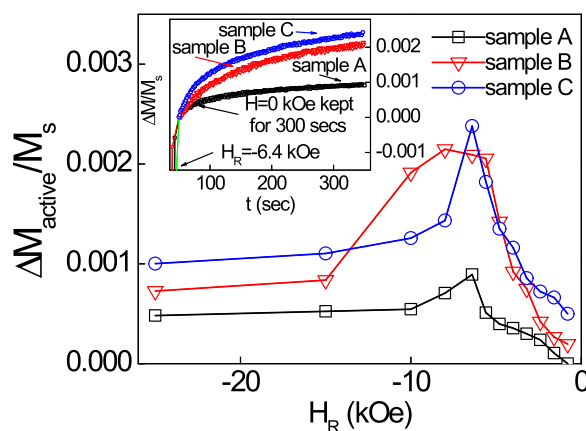
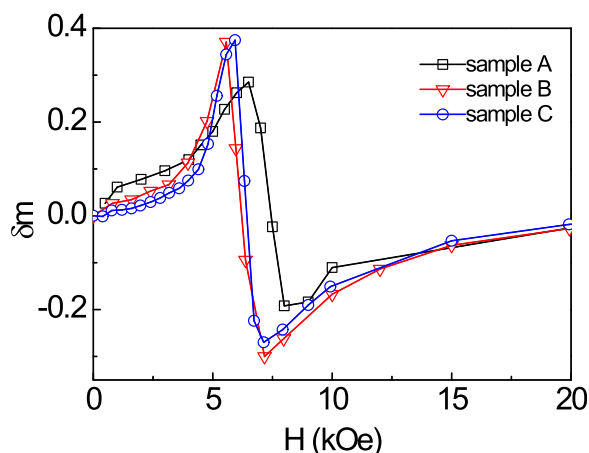


FIG. 2. The field H_R dependences of the value of magnetization reversal in the process of keeping the field fixed at zero for 300 s in samples A, B, and C at the temperature of 300 K, and the inset shows the process of magnetic relaxation after the field is cycled from -6.4 kOe.

magnetization reversal, the nucleation of reversed domain is necessary,^{32,36-38} and in the magnetic relaxation a thermally activated nucleation is transferred into hard grain surface, which is due to that the energy barrier is reduced by the isotropic exchange coupling and overcome with the driving of thermal fluctuation,^{20,38,39} subsequently leading to the depinning and free propagation of domain wall within the hard grain. Therefore, although the thermal activation involves magnetization reversal in soft grains, it originates from magnetization reversal in hard grains owing to the exchange coupling at hard grain interface.²⁰ The magnetization reversal of soft grain follows that of the neighboring hard grains, and consequently amplifies the value of thermal activation.^{20,40}

Bearing these in mind, we can speculate the exchange coupling effect at hard grain interface in these samples. For samples B and C, the significant thermal activation involves the reversible magnetization reversal in hard grains, indicating that the magnetocrystalline anisotropy energy in hard grains is overcome by exchange coupling energy with the driving of thermal fluctuation, which owes to the intrinsic exchange coupling effect at hard grain interface. For sample A, the thermal activation of magnetization reversal is less significant, and so magnetization reversal occurs less possibly in hard grains, which implies a decoupled effect between hard-hard grains.

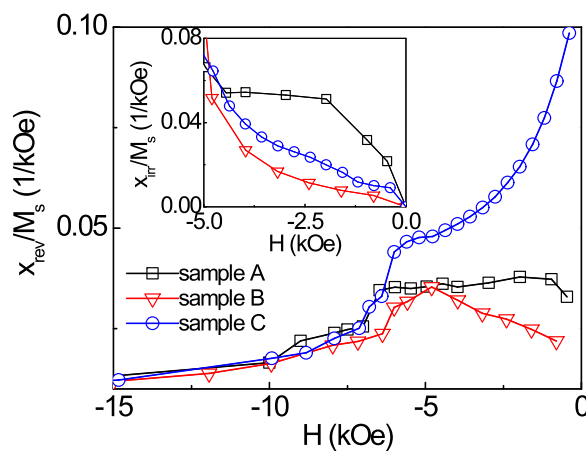
The exchange coupling at hard grain interface involves that not only between hard-hard grains but also between soft-hard grains, and because of the exchange coupling between soft-hard grains the thermal activation of magnetization reversal also involves that of soft grains. So the exchange coupling effect is necessary to be further investigated in these samples. Henkel plots (δm curve) are used to check the exchange coupling effect, which are defined as $\delta m = [2M_r(H) + M_d(H)]/M_r - 1$.^{21,22} Here, $M_r(H)$ is the remanence which is obtained by applying and the subsequent removal of a positive field H , M_r is the remanence for the sample magnetized to saturation, and $M_d(H)$ is the remanence by applying and the subsequent removal of a negative field H on the sample after magnetized to saturation. It can be seen in Fig. 3 that the peaks on δm curves are nearly the same for samples B and C, but lower for sample A. The

FIG. 3. δm curves for samples A, B, and C.

positive δm value indicates that exchange interaction is dominant over dipolar interaction. According to these facts, it seems that the exchange coupling effect is strong both in samples B and C, but weak in sample A. Actually, in the formula $\delta m = [M_d(H) + 2M_r(H)]/M_r - 1$, $M_r(H)$ and $M_d(H)$ are the remanences which are irreversible magnetization, and the irreversible magnetization results from the magnetization in hard grains. So it is more reasonable to say that δm could check the exchange coupling effect directly between hard-hard grains rather than between soft-hard grains.¹⁷ So according to the δm curves, the decoupled effect is confirmed between hard-hard grains in sample A, and the exchange interaction is evident between hard-hard grains in samples B and C. However, for sample C, since the squareness of demagnetization curve deteriorates, the exchange coupling effect is weak between soft-hard grains, which owes to the less content of hard phase and more content of residual interfacial amorphous phase.

In nanocomposite magnets, reversible magnetization reversal mainly originates from the effect of exchange coupling, and irreversible magnetization results from magnetization reversal in hard grains.¹⁷ For understanding fully the intergranular exchange effect, we investigate the reversible susceptibility χ_{rev}/M_s and irreversible susceptibility χ_{irr}/M_s in these samples (shown in Fig. 4). At the field lower than the coercive field, for sample C, the magnetization is the most reversible, suggesting the exchange interaction existing in the over melt-spun ribbons. For sample A, the magnetization is more reversible than that for sample B at low demagnetizing field, which should be attributed to the exchange coupling between soft-hard grains in the under melt-spun ribbons. However, as seen in the inset of Fig. 4, the irreversible magnetization is the most dominant at low demagnetizing field for sample A, indicating a weak resistance against magnetization reversal in some hard grains and the decoupled effect between hard-hard grains.

Bearing these facts in mind, the intergranular exchange coupling effect is much clear in the samples. For sample A, due to the decoupled effect between hard-hard grains, magnetization reversal occurs more probably in hard grains at low demagnetizing field. This magnetization reversal is more irreversible, and so the thermal activation of magnetization reversal is less dominant in the magnetic relaxation

FIG. 4. The reversible susceptibility χ_{rev}/M_s versus the field for samples A, B, and C at the temperature of 300 K, and the inset shows irreversible susceptibility χ_{irr}/M_s versus the field.

process. It is worthwhile to note that soft grains are coupled with hard grains, so the reversible magnetization is evident in sample A. For samples B and C, owing to the exchange coupling at hard grain interface, it is that in some hard grains magnetization reversal is also reversible, and so the thermal activation is dominant. However, for sample C, it is noted that, due to the less content of hard phase and more content of amorphous phase, the exchange coupling strength is weak between soft-hard grains and the resistance against magnetization reversal is weak in some grains, even though the intrinsic coupling strength is strong at hard grain interface and the magnetization reversal is more reversible.

In summary, even with a rather complicated feature the intergranular exchange coupling effect could be investigated via different angles, i.e., the thermal activation, Henkel plots and the susceptibilities. According to the investigations, it becomes much clear about the nature of exchange coupling between hard-hard grains and between soft-hard grains in under, optimal and over melt-spun ribbons. It is expected that these investigations may contribute to a better understanding of the exchange coupling effect in nanocomposite magnets.

The present work was supported by the Knowledge Innovation Project of the Chinese Academy of Sciences and the National Basic Research Program of China (Grant No. 2014CB643702).

¹R. Skomski and J. M. D. Coey, *Phys. Rev. B* **48**, 15812 (1993).

²J. Bauer, M. Seeger, A. Zern, and H. Kronmüller, *J. Appl. Phys.* **80**, 1667 (1996).

³J. Zhang, S. Y. Zhang, H. W. Zhang, B. G. Shen, and B. H. Li, *J. Appl. Phys.* **89**, 2857 (2001).

⁴W. Liu, Z. D. Zhang, J. P. Liu, Z. R. Dai, Z. L. Wang, X. K. Sun, and D. J. Sellmyer, *J. Phys. D: Appl. Phys.* **36**, L63 (2003).

⁵E. E. Fullerton, J. S. Jiang, C. H. Sowers, J. E. Pearson, and S. D. Bader, *Appl. Phys. Lett.* **72**, 380 (1998).

⁶J. P. Liu, in *Nanoscale Materials and Applications*, edited by J. P. Liu, E. Fullerton, O. Gutfleisch, and D. J. Sellmyer (Springer, Berlin, 2009), p. 309.

⁷D. Goll, M. Seeger, and H. Kronmüller, *J. Magn. Magn. Mater.* **185**, 49 (1998).

⁸J. Unguris, R. J. Celotta, and D. T. Pierce, *Phys. Rev. Lett.* **67**, 140 (1991).

⁹X. Y. Zhang, Y. Guan, and J. W. Zhang, *Appl. Phys. Lett.* **80**, 1966 (2002).

- ¹⁰S. D. Li, B. X. Gu, H. Bi, Z. J. Tian, G. Z. Xie, Y. J. Zhu, and Y. W. Du, *J. Appl. Phys.* **92**, 7514 (2002).
- ¹¹D. T. Ngo, H. G. Duong, H. H. Nguyen, C. Nguyen, M. Basith, and D. Q. Hoang, *Nanotechnology* **20**, 165707 (2009).
- ¹²B. Lu, M. Q. Huang, Q. Chen, B. M. Ma, and D. E. Laughlin, *J. Magn. Magn. Mater.* **195**, 611 (1999).
- ¹³Y. Choi, J. S. Jiang, Y. Ding, R. A. Rosenberg, J. E. Pearson, S. D. Bader, A. Zambano, M. Murakami, I. Takeuchi, Z. L. Wang, and J. P. Liu, *Phys. Rev. B* **75**, 104432 (2007).
- ¹⁴W. Li, L. Li, X. H. Li, H. Y. Sun, and X. Y. Zhang, *J. Phys. D: Appl. Phys.* **41**, 155003 (2008).
- ¹⁵T. Zhao, Q. F. Xiao, Z. D. Zhang, M. Dahlgren, R. Grössinger, K. H. J. Buschow, and F. R. de Boer, *Appl. Phys. Lett.* **75**, 2298 (1999).
- ¹⁶J. S. Jiang, J. E. Pearson, Z. Y. Liu, B. Kabius, S. Trasobares, D. J. Miller, S. D. Bader, D. R. Lee, D. Haskel, G. Srajer, and J. P. Liu, *Appl. Phys. Lett.* **85**, 5293 (2004).
- ¹⁷Z. B. Li, M. Zhang, B. G. Shen, and J. R. Sun, *Appl. Phys. Lett.* **102**, 102405 (2013).
- ¹⁸K. V. O'Donovan, J. A. Borchers, C. F. Majkrzak, O. Hellwig, and E. E. Fullerton, *Phys. Rev. Lett.* **88**, 067201 (2002).
- ¹⁹Y. Choi, J. S. Jiang, J. E. Pearson, S. D. Bader, and J. P. Liu, *Appl. Phys. Lett.* **91**, 022502 (2007).
- ²⁰Z. B. Li, B. G. Shen, and J. R. Sun, *J. Appl. Phys.* **113**, 013902 (2013).
- ²¹O. Henkel, *Phys. Status Solidi* **7**, 919 (1964).
- ²²P. E. Kelly, K. O'Grady, P. I. Mayo, and R. W. Chantrell, *IEEE Trans. Magn.* **25**, 3881 (1989).
- ²³E. F. Kneller and R. Hawig, *IEEE Trans. Magn.* **27**, 3588 (1991).
- ²⁴E. P. Wohlfarth, *J. Phys. F: Met. Phys.* **14**, L155 (1984).
- ²⁵P. Gaunt, *J. Appl. Phys.* **59**, 4129 (1986).
- ²⁶R. Street and S. D. Brown, *J. Appl. Phys.* **76**, 6386 (1994).
- ²⁷C. Rong, Y. Liu, and J. P. Liu, *Appl. Phys. Lett.* **93**, 042508 (2008).
- ²⁸H. W. Zhang, S. Y. Zhang, B. G. Shen, D. Goll, and H. Kronmüller, *Chin. Phys. Lett.* **10**, 1169 (2001).
- ²⁹H. Kronmüller and M. Fähnle, *Micromagnetism and the Microstructure of Ferromagnetic Solids* (Cambridge University Press, 2003), p. 420.
- ³⁰V. M. T. S. Barthema, D. Givord, M. F. Rossignol, and P. Tenaud, *J. Magn. Magn. Mater.* **242**, 1395 (2002).
- ³¹Y. Gao, D. Shindo, and A. K. Petford-Long, *J. Appl. Phys.* **93**, 8119 (2003).
- ³²Z. B. Li, B. G. Shen, E. Niu, and J. R. Sun, *Appl. Phys. Lett.* **103**, 062405 (2013).
- ³³H. Kronmüller and D. Goll, *Physica B* **319**, 122 (2002).
- ³⁴G. P. Zhao, X. L. Wang, C. Yang, L. H. Xie, and G. Zhou, *J. Appl. Phys.* **101**, 09K102 (2007).
- ³⁵D. Goll and H. Kronmüller, *Physica B* **403**, 1854 (2008).
- ³⁶H. Kronmüller, K.-D. Durst, and M. Sagawa, *J. Magn. Magn. Mater.* **74**, 291 (1988).
- ³⁷X. C. Kou, H. Kronmüller, D. Givord, and M. F. Rossignol, *Phys. Rev. B* **50**, 3849 (1994).
- ³⁸D. Givord, M. Rossignol, and V. M. T. S. Barthem, *J. Magn. Magn. Mater.* **258**, 1 (2003).
- ³⁹D. Givord, P. Tenaud, and T. Viadieu, *IEEE Trans. Magn.* **24**, 1921 (1988).
- ⁴⁰B. Zheng, H. W. Zhang, S. Zhao, J. Chen, and G. Wu, *Appl. Phys. Lett.* **93**, 182503 (2008).